Performance Comparison of Wavelet Families for DWT-Based Fusion of CT & MRI Images

Diana Madrid

October 26, 2021

Performance Comparison of Wavelet Families for DWT-based Fusion of CT & MRI Images

Diana Madrid
UNITEC
Tegucigalpa, Honduras
mail: letitbleed@unitec.edu

Abstract—**Research about image fusion has grown in the last three decades, essentially because there's a need to improve the data used for computerized post-processing and human visualization, being medical imaging a natural application for it. One of the latest used algorithms is the discrete wavelet transform (DWT) that is used for the analysis of non-stationary signals or those with discontinuities. Nevertheless, there are several wavelets that can be used as bases over which to do the transform. The preference of one over the other is determined experimentally and is heavily dependent on the application; in this case, the fusion of images obtained by magnetic resonance and computerized tomography. The fusion process with the 2D-DWT was done on MATLAB 9.3 CLI, using three pairs of slices for one, two, three and four levels of decomposition. The tested wavelets are symlet5, daubechies5 and discrete Meyer. The symlet5 filters showed the best (higher) mutual information (with superiority of ~0.07%) for all slices and almost all levels of decomposition except for level 2, in which discrete meyer wavelets were superior by 0.17%. For every pair of slices, symlet5 showed the best (lower) joint entropy. The results can be ascertained for T2 MRI and CT images.**

Keywords—DWT; Image fusion; Computed tomography; Magnetic resonance imaging

I. INTRODUCTION

The adoption of digital signal processing in the healthcare industry has been allowed due to the great degree of accuracy, affordability and speed achieved by the imaging technology and by the interpretation abilities spread by the health professionals. Amidst all the developed modalities, the most popular are the tomographic ones, particularly CT and MRI images, because of the complementary anatomic information they provide. Simple visualization of both image modalities in one can be achieved by register and blending techniques; fusion, on the other hand, is desirable for classification and tumor detection, registering the progress of a disease, tracking of brachytherapy devices, surgery planning, voxel fusion, intensity- and object-based segmentation and 3D simulations.

Some of the most recent algorithms are the DWT-based ones, which allow the separation of the image in frequency bands, each one with different details, which eases extraction of border information, compression, transmission, and noise-reduction. For image treatment, variations of the 1D DWT have been developed. 2D-DWT has been shown to keep more spectral content of the source images, up to 85%, in contrast with conventional techniques like IHS, Brovey transform and PCA, which keep 43%, 53% and 62.5% respectively [14]. The problem lies in the fact that the superiority of one wavelet family over another cannot be determined solely by inspection of it but is determined greatly by the nature of the signal being analyzed; thus, the need to specify a wavelet for each signal, being CT-MRI fusion an application that must not be ignored.

II. WAVELET TRASFORM

A. Continuous wavelet transform

The continuous wavelet transform (CWT) is developed as a response to the problem of representing signals with discontinuities in the frequency domain, particularly because the Fourier Transform uses sines and cosines which are smooth, analytic, and infinite and may not characterize properly erratic real signals. The CWT is implemented, as many other transforms, as the inner product of the signal and the base function, in the following manner:

$$CWT(s,\tau) = \langle \psi_{s,\tau}, s(t) \rangle = \frac{1}{\sqrt{s}} \int_{-\infty}^{\infty} s(t)\, \psi^* \left(\frac{t-\tau}{s} \right) dt \quad (1)$$

Where the signal to be represented is s(t), * denotes the complex conjugate and CWT is the coefficient of the expansion. It has the property of multiresolution representation, which means that, through the factor *s,* the wavelet may be stretched or compressed, allowing for different scales. With the factor τ the wavelet basis can be translated in position with respect to the signal and thus obtain a more detailed description.

B. Discrete wavelet transform

There are three main issues in the implementation of the CWT, pointed out by Valens [3]. Because each scaling s and slide τ is a continuous value, the number of wavelet coefficients obtainable is theoretically limitless. It also suffers from the redundancy of mapping a signal in one variable, t, to two variables, s and τ. Finally, the CWT as introduced in (1), has only numerical solutions, when what is needed for the implementation are fast algorithms. To solve the redundancy issue, there are critical sampling values, which will reduce the number of translations and dilations to the minimum needed for reconstruction. These turn out to be values in octave or in dyadic scaling [2], as shown in (2).

$$\psi_{j,k}(t) = \frac{1}{\sqrt{2^j}} \, \psi(2^{-j}t - k) \qquad (2)$$

Moreover, this high pass filter —limited in the upper bound by the frequency content of the signal— has the disadvantage that whenever it is stretched in the time domain by a factor of 2, its bandwidth is reduced by the same factor, thus being unable to properly cover the signal's content down to the 0-frequency component. Hence the need of a low pass filter, called the father wavelet or scaling function ϕ, which provides the approximation or scaling coefficients of the transform, while ψ provides the detail or wavelet coefficients. The representation of ϕ is analogous to the one in (2), while the transform is directly obtained as in (3).

$$f(t) = \sum_k a_{j0}(k)\varphi_{jo,k}(t) + \sum_{j=j0}^{\infty} \sum_k d_j(k)\psi_{j,k}(t) \qquad (3)$$

In the above equation, k is the translation parameter, j is an arbitrary resolution level or scale in which one would want to examine the signal and $a_{j\,(k)}, d_j(k)$ are the approximation and detail coefficients, respectively. They are obtained as per the properties of orthogonal bases [12], with the inner product of the bases and the signal of interest f(t), i.e., calculating the transform itself:

$$a_{j-1}(k) = \langle f(t), \varphi_{j,k}(t) \rangle ; \; d_{j-1}(k) = \langle f(t), \psi_{j,k}(t) \rangle$$

C. Fast wavelet transform

With the above discretization, the transform is easier to obtain since the wavelet and scaling functions can be implemented as filter taps, but it is nevertheless computationally expensive. Mallat [12] showed that the wavelet transform can be represented as with multiresolution analysis, meaning that each resolution or scale can be represented in terms of the previous scale, being the scale j a subspace of scale j+1. Equation 5 shows that it is possible to calculate any coefficient of greater level by doing the convolution of the approximation coefficient of the level before with the high pass and low pass filter points —h and g, respectively—, sparing the need to calculate the inner product for each approximation and detail coefficient with the signal.

$$a_k^{(j+1)} = \sum_n h_{n-2k}a_n^{(j)} \quad d_k^{(j+1)} = \sum_n g_{n-2k}a_n^{(j)} \qquad (5)$$

III. IMAGE FUSION ALGORITHM

The fusion process is done directly on the wavelet domain, wherein the coefficients of each frequency band must be fused with the corresponding coefficients of the other image. Up to the moment the transform has been expressed for one-dimensional signals, so now an expansion to two dimensional signals must be done. A schematic of the process is shown in **Fig. 1**.

A. Analysis

The signal of interest is an image, which is composed of rows and columns of a finite size. For two dimensions, then, a similar algorithm to the one-dimensional case can be used, in which the scaling (low-pass) and wavelet (high-pass) filter must be applied successively to rows and to the columns. In the analysis process, each low and high pass filter cut the frequency band of the signal in half, which means that the number of samples needed to represent it are less; particularly, half the number of original samples, as per the sampling theorem.

Successive filtering must be applied for the rows and columns in all the different permutations, namely: low-pass filter the rows and then low-pass the columns; low-pass filter the rows and high-pass filter the columns; high-pass filter the rows and low-pass filter the columns; and high-pass filter both rows and columns. The result of this four-filtering process are four different frequency bands, as in Fig. 1, wherein the low-low filtered band corresponds to an approximation or lower size version of the original image, and the other bands give the vertical, horizontal, and diagonal details, respectively. Doing this process once yields the first level of analysis or
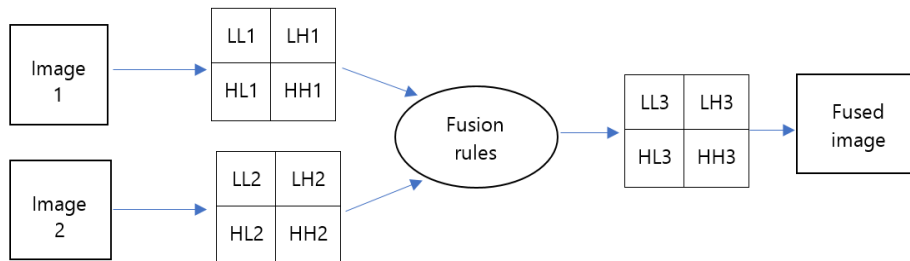

Fig. 1. Schematic of fusion process using DWT

decomposition, while repeatedly doing this process on the approximation band of the previous level results in more levels of analysis, with a total of 3N+1 bands, where the +1 corresponds to the approximation band of the first level.

B. Fusion rules

Any fusion process needs to decide how to merge, what parts to keep and how to modify the original data into only one. Since the fusion process using DWT is done on the transform domain, the easiest approach is to merge using simple arithmetic rules, like to keep the coefficient of smaller value in a pixel or to average the values. The maximum value rule strives to keep the coefficient of greater value, which should, in turn, mean that there is a high correlation of the original signal with the high "frequency" wavelet, and is useful to keep the details of any of the original data sequences, since high frequency components are related to abrupt changes in intensity, signaling a border or detail.

C. Synthesis

The synthesis process, posterior to the coefficient's fusion, is the exact reverse of the analysis process. It is necessary to up-sample the coefficients by the same factor by which it was decimated, namely a factor of two. Then the corresponding low-pass and high-reconstruction filters are applied on columns and rows the same number of times (N levels).

IV. QUALITY ASSESSMENT

All fusion methods strive to preserve spectral content and perhaps increase resolution without introducing, and even eliminating, artifacts and inconsistencies. The main difficulty lies in defining a criterion for quantitative assessment because there's not an ideal fused image reference to compare the results with. For the medical image fusion application, the goal is to maintain the soft tissue information of the MRI and the clear bone tissue information provided by the CT image.

A. Qualitative evaluation

The qualitative evaluation is to be done through visual inspection and appreciation of a medical and tech team. The quality is to be compared both between the fused images themselves and with the original images, using parameters such as spatial detail, resolution, geometric patterns, color, etc. Of course, this method doesn't rely on numerical models and is mainly dependent on the observer's experience, being that its main disadvantage.

B. Entropy and Mutual Information

The entropy of a discrete random variable X with a probability distribution p(x) is defined as:

$$H(X) = -\sum_x p(x) \log p(x) \qquad (6)$$

It indicates the average information contained in an image [4], in such a way that if the intensity value of the

image is equal for all pixels, p(x)=1 and entropy is zero; and if the probability of a pixel intensity is very low, it means that it is a very 'meaningful' event, and the entropy is higher. To know the information conveyed by two random variables X and Y, joint entropy is used. To calculate it, similarly to (6), one must find the joint probability distribution p(x, y). If the joint entropy is low, then uncertainty between two images is low too.

$$H(X, Y) = -\sum_{x \in X} \sum_{y \in Y} p(x, y) \log p(x, y) \qquad (7)$$

From joint entropy, mutual information (MI) is calculated as the Kullback-Leibler divergence of the product of the marginal distributions p(x) and p(y) from the joint distribution p(x, y). It reflects how much uncertainty is reduced in a variable due to the knowledge of the other one.

$$I(X; Y) = \sum_{x \in X} \sum_{y \in Y} p(x, y) \log \frac{p(x,y)}{p(x)p(y)} \qquad (8)$$

In relation to image fusion evaluation, joint entropy should indicate the similarity of the fused image with the original signals, if there were no artifacts introduced in the fusion process; the lower it is, the "better" it should be. On the other hand, the higher MI is, the better a pixel x predicts the value of the corresponding pixel y; it evaluates both the wavelet's and the fusion algorithm's quality. It should be noted from (7) and (8) that the computation of mutual information involves the computation of joint entropy.

V. IMPLEMENTATION

The MRI brain images used were obtained in axial direction and belong to T2 weighting, with a thickness of 5 mm, repetition time of 5000 ms and echo time of 105.4 ms. Specifically, the fast recovery fast spin echo (FRFSE) sequence was used since it showed great contrast to noise ratio and just a small deterioration in signal to noise ratio despite the big matrix size (512x512). The CT slices chosen had a thickness of 0.6 mm, with 439 mA, 120 KVp and standard reconstruction kernel. They were converted from RGB to grayscale for easier processing. The slice positions (SP) pairs are shown in Table I. **Fig.2** and **Fig. 3** show original data sets for a SP of 78 mm.

TABLE I.   DOMAIN OF SOURCE IMAGES

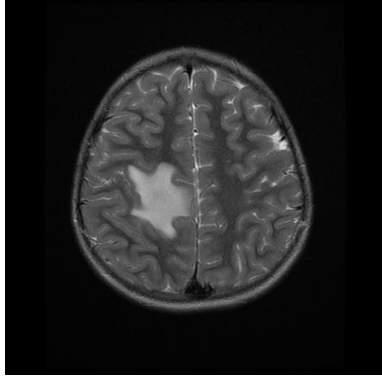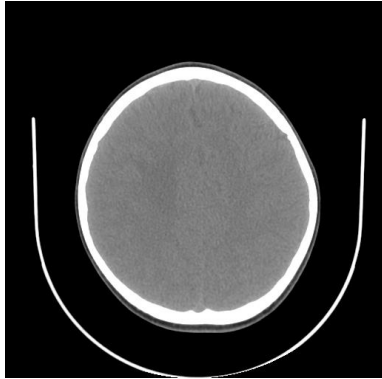| Pair number	Slice position (mm)	
	CT	**MRI**
1	7.125	7.142
2	50.875	51.121
3	78.375	78.608

Fig.2. MRI T2-weighted image at SP 78 mm

Fig.3. CT image at SP 78mm

A. MATLAB

MATLAB is a programming environment based on C, C++ and Java that works with data arranged as matrices. It is useful to manipulate and perform mathematical operations on big amounts of data, to implement numerical analysis algorithms, to do plots and to develop graphical interfaces. Its latest stable release is MATLAB R2018a, available for Windows, macOS and Linux. It possesses toolboxes and predetermined functions, among which are the Wavelet Toolbox and the Image Processing Toolbox, with their functions to do 1D & 2D-DWT and to import dicom images, which is the standard for medical images.

B. Joint entropy and MI algorithm

For the calculation of mutual information, the feature mutual information algorithm was chosen, in its fast-mutual information variant published in [5], with no feature extraction parameters selected. This algorithm takes as input the original two images and the fused one, then it calculates the two MIs and averages them. The result is normalized to yield a maximum of 100%. For the joint entropy, the calculus of joint histogram provided by [8] was used. For reference, the joint entropy of a CT image with itself is in the range of 3.0846 to 3.4512, and of an MRI with itself is in between 5.0646 and 5.4610, while MI of an image with itself and a CT one doesn't exceed 93.67%, for the present input data.

C. Image Registration

Image registration was done using MATLAB intensity-based image registration function [7], which already suggests an optimizer and metric for the case of multimodal image registration. The parameters of the metric —which uses Bayes mutual information— were taken from the *multimodal* default settings, while the parameters for the optimizer (OnePlusOneEvolutionary) were modified as to avoid local maxima of mutual information for both images and to guarantee convergence of the algorithm, shown in Table II. The transform type allowed was limited to rigid since the images follow the positioning protocol that guarantees parallelism among slices. The superimposed original images and the result of the registration are shown in *falsecolor* mode on **Fig. 4** and **Fig.5**, respectively, for a SP of 78 mm.

TABLE II. OPTIMIZER PARAMETERS

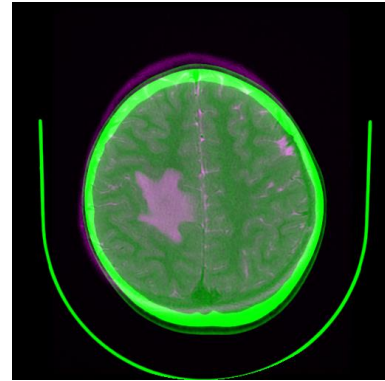| Parameters	Values
Initial Radius	0.010
Minimal radius	1.008e-8
Iteraciones máximas	700
Factor de crecimiento	1.0001

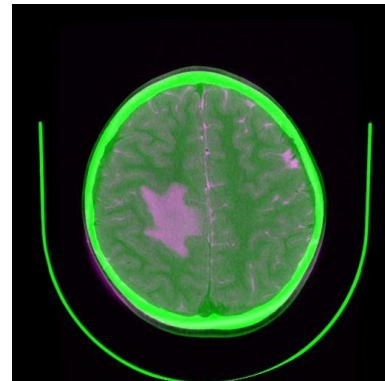**Fig. 4.** Falsecolor superimposed original slices

Fig. 5. Falsecolor superimposed registered slices

D. Wavelet families

The term wavelet family refers to the pair of scaling φ and wavelet ψ filters, which are inherently related to

each other by a time reversal and an alternating sign, conforming quadrature mirror filters [11]. When the data to be analyzed is decomposed using DWT, the adequate representation of the characteristics of the signal depends on the shape of the wavelet. The coefficients generated by the best suited filter family should represent a more faithful feature and detail extraction, because while more modifications are inflicted upon the original coefficients –as in an image fusion process— the more the reconstruction quality will depend on the inherent properties of φ y ψ filters.

In different papers, different wavelet families showed the best performance for the fusion of MRI & CT images: symlet [1], daubechies [10] and discrete meyer [6]. The daubechies family was designed for maximum number of vanishing moments for a given support; the symlet was designed similarly, with special emphasis on achieving symmetry; and the discrete meyer is a discretization of an originally continuous and infinitely differentiable wavelet. Both the symlet and daubechies are compactly supported orthonormal wavelets; filters of 10 points (order 9) were chosen for computational ease and because of the good experimental results observed. For the filters' design, MATLAB's default db5, sym5 and dmey wavelets were selected.

VI. RESULTS

The three pairs of images were fused for levels 1, 2, 3 and 4 for all three selected wavelet families: discrete meyer, daubechies with 5 vanishing moments and symlet 5, as well.

A. Fusion algorithm

Validation of the performance of the decomposition and reconstruction process was done using an ad hoc blurred gray scale picture, as to simulate multifocal image fusion, shown in **Fig. 6** for the dmey family.
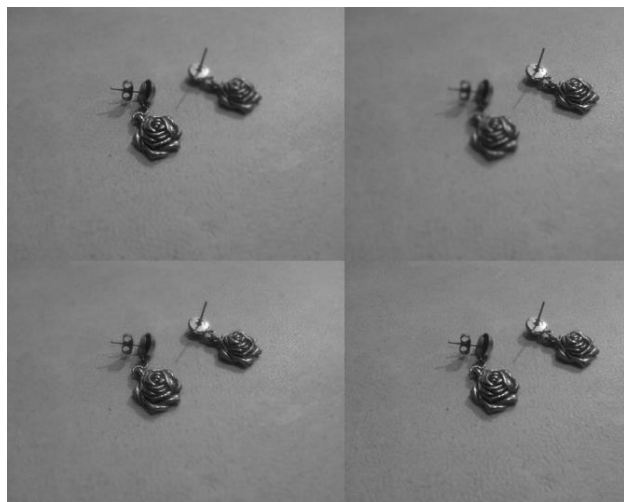

Fig. 6. Original multifocal pictures (top row). DWT fused image (bottom left row) and original unblurred picture.

B. Quantitative comparison

MI turned out to be greater (0.17%) for levels 1, 3 and 4 in the fusion done with the symlet wavelet, being this behavior consistent for all SPs. In level 2, MI for the discrete meyer wavelet was significantly higher (0.17%) than the symlet's. Joint entropy was, similarly, lower for the symlet family in all levels and slices. The resulting fusion for all levels is shown in Table III (next page) for the data at SP 78 mm. There is a noticeable decline in MI for increasing levels, as well as an increasing joint entropy. This is due to the increasing presence of high frequency artifacts, that probably stem from the quantization process, the DWT limitations [8], and aliasing arising from the disturbance —i.e., the fusion process— in the QMF balance.

C. Qualitative assessment

Four doctors, four radiology practitioners and four radiology technicians were interviewed about the outcomes of the fusion process. The doctors mentioned that they did not notice a significant difference between each family for a given level, while the radiology technicians preferred in 50% of the samples the result given by the symelt family, choosing other family randomly the other half of the time, mentioning that they didn't notice any significant difference in resolution and contrast. The radiology practitioners all immediately choose the symlet family as the preferred one, because it looked "more real". This judgement is probably related to the gray scale fidelity of the fused images to the original ones, thus providing a different and valuable criterion from someone exposed daily to this type of signals.
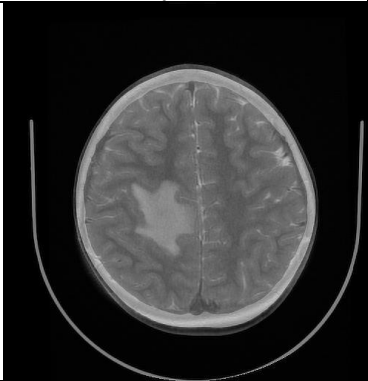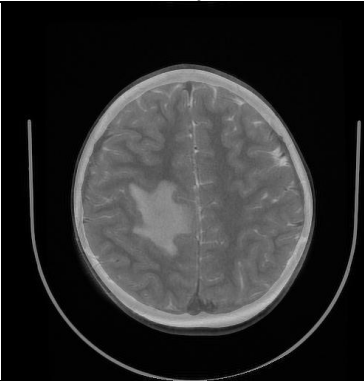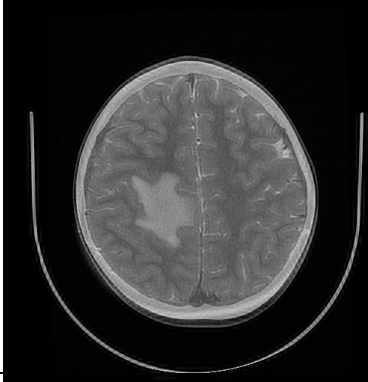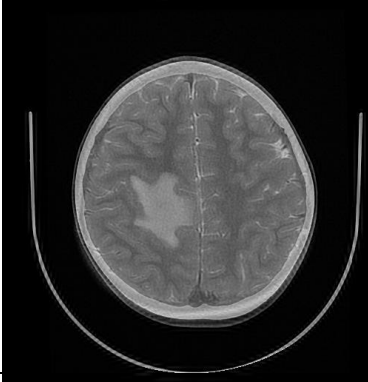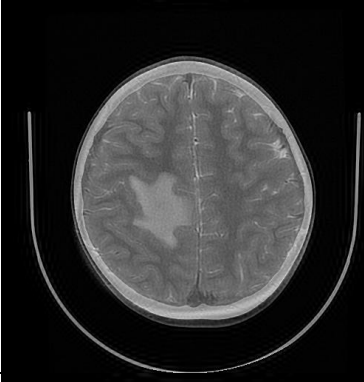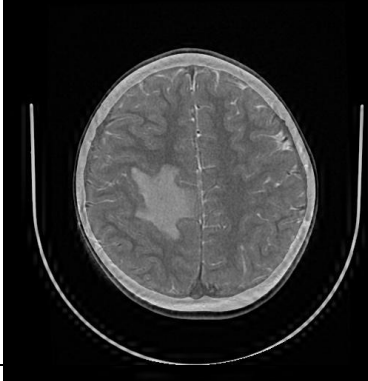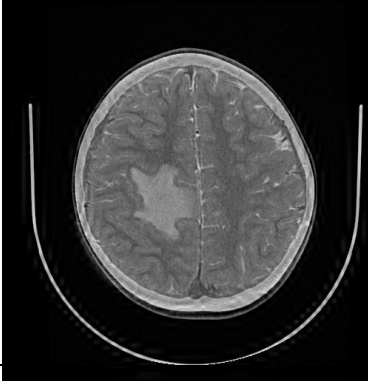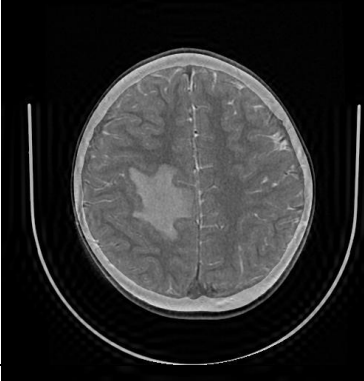
REFERENCES

[1] B. Renuka and A. Hasan, "Fusion of medical images in MATLAB using different wavelet parameters," *International Journal & Magazine of Engineering, Technology, Management and Research,* vol. 3, no.12, pp.595-600, 2016 [Online]. Available: http://www.ijmetmr.com/oldecember2016/BRenuka-AliyaHasan-83.pdf [Accessed: May 28, 2018]

[2] B. Vidakovic, "Basics of Wavelets," 2004. [Online]. Available: https://b.gatech.edu/2ksk7r8. [Accessed: May 27, 2018]

[3] C. Valens, "A Really Friendly Guide to Wavelets," 1999 [Online]. Available: http://citeseerx.ist.psu.edu/viewdoc/summary ?doi=10.1.1.34.2

[4] D.-Y. Tsai, Y. Lee and E. Matsuyama, "Information Entropy Measure for Evaluation of Image Quality," *Journal of Digital Imaging,* vol. 21, no. 3, pp.338-347, 2008. doi: 10.1007/s10278-007-9044-5.

[5] M. Haghighat and M. Amirkabiri, "Fast-FMI: Non-reference image fusion metric," 2014 IEEE 8th International Conference on

Application of Information and Communication Technology (AICT)," [Online]. Available: https://ieeexplore.ieee.org/document/7036000/

[6] N. Mittal and R. Gupta, "Fusion of MRI & CT medical images with different wavelet transforms using wavelet method," *Apeejay - Journal of Management Sciences & Technology,* vol.2, no. 3, pp.15-21, 2015 [Online]. Available: http://apeejay.edu/aitsm/journal/docs/issue-june-2015/ajmst020303.pdf. [Accessed: May 28, 2018]

[7] "Imregister," MATLAB, 2012. [Online] Available: https://bit.ly/2Lz8hYI

[8] I. Selesnick, R. Baraniuk, and N. Kingsbury, "The Dual-Tree Complex Wavelet Transform," *IEEE Signal Processing Magazine,* vol. 22, no. 6, pp. 123-151, 2005 [Online]. Available: https://ieeexplore.ieee.org/document/1550194/

[9] P. Mahmoudzadeh, "Joint histogram (x, y)," *Mathworks,* 2016. [Online]. Available: https://bit.ly/2LzHPhz

[10] R. Bhandari and B. Shivakumar, "Wavelet based analysis of medical image fusion using MATLAB GUI," *International Journal of Innvative Research in Science, Engineering and Technology,* vol. 5, pp.512-517, 2016 [Online]. Available: https://bit.ly/2kwax6Q. [Accessed: May 28, 2018]

[11] S. Agrawal and O. Sahu, "Two-channel quadrature mirror filter banks: An overview," *ISRN Signal Processing,* vol. 2013, [Online]. Available: http://dx.doi.org/10.1155/2013/815619

[12] S. Mallat, "A theory for multiresolution signal decomposition: the wavelet representation," *IEEE Transactions on Pattern Analysis and Machine Intelligence*, vol. 11, no.7, pp. 674-693, 1989 [Online]. Available: https://ieeexplore.ieee.org/document/192463/

[13] S. Mallat, *A wavelet tour of signal processing.* Burlington, MA, USA: Elsevier, 2009 [Online]. Available: https://bit.ly/2L1WxwO. [Accessed: May 27, 2018]

[14] S. Sanjeevi, K. Vani and K. Lakshmi, "Comparison of Conventional and Wavelet Transform Techniques for Fusion of IRS-1C LISS III and PAN Images," in 22nd Asian Conference on Remote Sensing, Tamil Nadu, 2001 [Online]. Available: https://bit.ly/2seLJo1. [Accessed: May 27, 2018]

TABLE III. FUSION RESULTS FOR CT AND MRI BRAIN SLICES

	Sym5	Db5	Dmey
1			
2			
3			
4			